

# Quantitative Method for the Profiling of the Endocannabinoid Metabolome by LC-Atmospheric Pressure Chemical Ionization-MS

John Williams,<sup>†,‡</sup> JodiAnne Wood,<sup>†</sup> Lakshmipathi Pandarinathan,<sup>†</sup> David A. Karanian,<sup>§</sup> Ben A. Bahr,<sup>§</sup> Paul Vouros,<sup>\*,‡</sup> and Alexandros Makriyannis<sup>\*,†</sup>

Center for Drug Discovery, and Department of Chemistry and Chemical Biology, Northeastern University, Boston, Massachusetts 02115. and Department of Pharmaceutical Sciences, University of Connecticut, Storrs, Connecticut 06269

The endocannabinoid system's biological significance continues to grow as novel endocannabinoid metabolites are discovered. Accordingly, a myopic view of the system that focuses solely on one or two endocannabinoids, such as anandamide or 2-arachidonoyl glycerol, is insufficient to describe the biological responses to perturbations of the system. Rather, the endocannabinoid metabolome as a whole must be analyzed. The work described here is based on liquid chromatography coupled with atmospheric pressure chemical ionization mass spectrometry. This method has been validated to quantify, in a single chromatographic run, the levels of 15 known or suspected metabolites of the endocannabinoid system in the rat brain and is applicable to other biological matrixes. We have obtained an endocannabinoid profile specifically for the frontal cortex of the rat brain and have determined anandamide level differences following the administration of the fatty acid amide hydrolase inhibitor AM374.

The endocannabinoid metabolome can be defined as the full complement of endogenous lipid signaling mediators that are associated with the endocannabinoid system. This metabolome's composition reflects physiological states (normal and pathological) known to be associated with the endocannabinoid system. The endocannabinoid system includes the CB1 receptor, found in high abundance in the hippocampus, cortex, cerebellum, and basal ganglia regions of the brain,<sup>1</sup> the CB2 receptor, found primarily in immune tissue,<sup>2</sup> and possibly a third cannabinoid receptor, CB3.<sup>3</sup> The first endogenous lipid agonist discovered to have high affinity to the CB1 receptor was anandamide (AEA), an *N*-acylethanolamide derivative of arachidonic acid.<sup>4</sup> Soon after, the monoacyl glyceride of arachidonic acid, 2-arachidonoyl glycerol

(2AG), was identified as an agonist to both CB1 and CB2 receptors.<sup>5</sup> The endocannabinoids are biosynthesized and biotransformed by a number of enzymes, leading to a variety of enzymatic products and intermediates, and many of these appear to play a role in modulating endocannabinoid-related physiological functions. Upon depolarization, induced  $\text{Ca}^{+2}$  influx endocannabinoids are released from postsynaptic neurons and act as retrograde synaptic messengers on CB receptors located on presynaptic neurons.<sup>6,7</sup> The endocannabinoid system is involved in many physiological processes, including antinociception, hypothermia, analgesia, and catalepsy.<sup>8</sup>

Following the discovery of AEA and 2AG, an effort has been underway to identify other lipids associated with the endocannabinoid system. For instance, several classes of lipid modulators found to interact both directly and indirectly with the endocannabinoid system are the *N*-acyl ethanolamides, acyl glycerols, acyl amides, and acyl amino acids.<sup>9</sup> The "focused metabolomic" approach has been successful largely due to advances in liquid chromatography–mass spectrometry (LC–MS) technology.<sup>10,11</sup> Recent developments using hybrid quadrupole time-of-flight mass spectrometers coupled to nanoLC have identified 40 novel acyl amino acid species with potential bioactivity.<sup>12</sup> In the *N*-acyl ethanolamide class, palmitoyl ethanolamide (PEA) is a known anti-inflammatory and antinociceptive agent whose effects are amplified synergistically when administered with AEA.<sup>13</sup> Oleoyl ethanolamide (OEA) has been shown to inhibit AEA uptake and degrada-

\* To whom correspondence should be addressed. E-mail: a.makriyannis@neu.edu. Tel.: 617-373-4200. Fax: 617-373-7493. E-mail: p.vouros@neu.edu. Tel.: 617-373-2840. Fax: 617-373-2693.

<sup>†</sup> Center for Drug Discovery, Northeastern University.

<sup>‡</sup> Department of Chemistry and Chemical Biology, Northeastern University.

<sup>§</sup> University of Connecticut.

(1) Tsou, K.; Brown, S.; Sanudo-Pena, M. C.; Mackie, K.; Walker, J. M. *Neuroscience* **1998**, *83* (2), 393–411.

(2) Munro, S.; Thomas, K. L.; Abu-Shaar, M. *Nature* **1993**, *365* (6441), 61–5.

(3) Breivogel, C. S.; Griffin, G.; Di Marzo, V.; Martin, B. R. *Mol. Pharmacol.* **2001**, *60* (1), 155–63.

(4) Devane, W. A.; Hanus, L.; Breuer, A.; Pertwee, R. G.; Stevenson, L. A.; Griffin, G.; Gibson, D.; Mandelbaum, A.; Etinger, A.; Mechoulam, R. *Science* **1992**, *258* (5090), 1946–9.

(5) Sugiura, T.; Kondo, S.; Sukagawa, A.; Nakane, S.; Shinoda, A.; Itoh, K.; Yamashita, A.; Waku, K. *Biochem. Biophys. Res. Commun.* **1995**, *215* (1), 89–97.

(6) Di, Marzo, V.; Melck, D.; Bisogno, T.; De Petrocellis, L. *Trends Neurosci.* **1998**, *21* (12), 521–8.

(7) Piomelli, D.; Beltramo, M.; Giuffrida, A.; Stella, N. *Neurobiol. Dis.* **1998**, *5* (6 Part B), 462–73.

(8) Palmer, S. L.; Thakur, G. A.; Makriyannis, A. *Chem. Phys. Lipids* **2002**, *121* (1–2), 3–19.

(9) Bradshaw, H. B.; Walker, J. M. *Br. J. Pharmacol.* **2005**, *144* (4), 459–65.

(10) Griffiths, W. J. *Mass Spectrom. Rev.* **2003**, *22* (2), 81–152.

(11) Han, X.; Gross, R. W. *J. Lipid Res.* **2003**, *44* (6), 1071–9.

(12) Tan, B.; Bradshaw, H. B.; Rimmerman, N.; Srinivasan, H.; Yu, Y. W.; Krey, J. F.; Monn, M. F.; Chen, J. S.; Hu, S. S.; Pickens, S. R.; Walker, J. M. *Aaps J.* **2006**, *8* (3), E461–5.

(13) Calignano, A.; La Rana, G.; Piomelli, D. *Eur. J. Pharmacol.* **2001**, *419* (2–3), 191–8.

tion,<sup>14</sup> in addition to regulating feeding behavior.<sup>15</sup> In the acyl glycerol class, 2-palmitoyl glycerol (2PG) does not bind directly to CB2 receptors but has been shown to increase the affinity of 2AG binding when coadministered in equal amounts.<sup>16</sup> The arachidonoyl glycerol ether, also called noladin ether, has CB1 activity and produces physiological responses similar to that of 2AG.<sup>17</sup> There are several other lipid modulators with known bioactivity, such as 2-linoleoyl glycerol and linoleoyl ethanolamide, that only differ from AEA and 2AG in the size of the acyl chain and the degree of unsaturation.<sup>9</sup>

Identifying novel lipid modulators must coincide with improved methods for their simultaneous quantitation in biological systems in order to evaluate the physiological changes that occur following administration of cannabimimetic agents. Initial efforts to quantify the *N*-acyl ethanolamides AEA, PEA, and OEA in rat plasma were performed by GC/MS.<sup>18</sup> This method required the time-consuming steps of prepurification and derivatization of the lipid extracts. Anandamide and 2AG were quantified in CB1 knockout mouse brain by a reversed-phase LC/MS method using atmospheric pressure chemical ionization (APCI).<sup>19</sup> Switching from GC to LC eliminated the need for derivatization, but prepurification steps were still used. Improving upon the original GC/MS method, Giuffrida introduced the first LC/MS method using electrospray ionization (ESI) to quantify AEA, PEA, and OEA in rat plasma, eliminating the prepurification and derivatization steps.<sup>20</sup> These methods all quantify by isotope dilution, using either the molecular ion  $[M + H]^+$  or the sodium adduct  $[M + Na]^+$  in selected ion monitoring (SIM) mode. A more sensitive and selective method of quantitation than the SIM mode is by selected reaction monitoring (SRM) mode using a triple-quadrupole mass spectrometer, in which only a single fragment ion from a single precursor is detected. Recently, an SRM-based quantitative LC/MS/MS method was developed to measure several derivatives of arachidonic acid, including AEA, 2AG, arachidonoyl glycine, arachidonoyl dopamine, and arachidonoyl  $\gamma$ -aminobutyric acid, in male and female rat brains.<sup>21</sup> A single internal standard, arachidonic acid-*d*<sub>8</sub>, was used as the internal standard based upon the common fatty acid core shared by all analytes. To date, this is the most comprehensive method available for the quantitative analysis of the arachidonic core-based endocannabinoids.

The purpose of this work is to develop and validate a robust, sensitive, and selective LC/MS/MS method for analyzing the endocannabinoid metabolome in biological matrixes. Here, the endocannabinoid metabolome has been expanded to include the

ethanolamide, glyceride, and free acid derivatives of six fatty acid core structures. The six fatty acid cores chosen were arachidonic (AA 20:4n6), docosahexaenoic (DHA 22:6n3), eicosapentaenoic (EPA 20:5n3), eicosenoic (EA 20:1n9), oleic (OA 18:1n9), and palmitic (PA 16:0) acids. Combined, the six fatty acids plus their corresponding glyceride and ethanolamide derivatives total 18 compounds that vary in size and degree of saturation. The choice of fatty acid cores is based upon evidence that the ethanolamide and glycerol derivatives are involved in the endocannabinoid system. In addition to the effects of OEA, PEA, and 2PG on the endocannabinoid system mentioned previously, docosahexaenoyl ethanolamide (DHEA) and 2-docosahexaenoyl glycerol (2DHG) have been identified in the bovine retina and are produced in a time-dependent manner with AEA.<sup>22</sup> In addition, DHEA and eicosapentaenoyl ethanolamide (EPEA) bind to the CB1 receptor in rat brains.<sup>23</sup> DHA levels in the mouse brain have been shown to inversely affect the levels of 2AG.<sup>24</sup> The role of EA, eicosenoyl ethanolamide (EEA), and 2-eicosenoyl glycerol (2EG) in the endocannabinoid system has not been established.

## EXPERIMENTAL SECTION

**Chemicals.** Arachidonylethanolamine and 2-arachidonoyl glycerol were gifts from the National Institute for Drugs of Abuse. Arachidonic, oleic, and docosahexaenoic acids were purchased from Nu-Check Prep (Elysian, MN). Oleylethanolamide, palmitic acid, palmitoylethanolamide, eicosapentaenoic acid, ACS grade acetone, 100 mM phosphate-buffered saline pH 7.4 (PBS), and HPLC grade ethanol were purchased from Sigma Aldrich (St. Louis, MO). Arachidonic acid-*d*<sub>8</sub>, docosahexaenoic acid-*d*<sub>5</sub>, eicosenoic acid, and eicosapentaenoic acid-*d*<sub>5</sub> were purchased from Cayman Chemical (Ann Arbor, MI). Palmitic acid-*d*<sub>4</sub> and oleic acid-*d*<sub>2</sub> was purchased from Cambridge Isotope Laboratories (Andover, MA). Arachidonylethanolamide-*d*<sub>4</sub>, 2-arachidonoyl glycerol-*d*<sub>5</sub>, oleylethanolamide-*d*<sub>4</sub>, 2-oleoyl glycerol, 2-oleoyl glycerol-*d*<sub>5</sub>, palmitoylethanolamide-*d*<sub>4</sub>, 2-palmitoyl glycerol, 2-palmitoyl glycerol-*d*<sub>5</sub>, docosahexaenylethanolamide, docosahexaenylethanolamide-*d*<sub>4</sub>, 2-docosahexaenoyl glycerol, 2-docosahexaenoyl glycerol-*d*<sub>5</sub>, eicosapentaenylethanolamine, eicopentaenylethanolamine-*d*<sub>4</sub>, 2-eicosapentaenoyl glycerol, 2-eicosapentaenoyl glycerol-*d*<sub>5</sub>, eicosenoic acid-*d*<sub>2</sub>, 2-eicosenoyl glycerol, 2-eicosenoyl glycerol-*d*<sub>5</sub>, eicosenylethanolamide, and eicosenylethanolamide-*d*<sub>4</sub> were synthesized in-house. The isotopic purity of each deuterated internal standard was greater than 98%, except for arachidonic acid-*d*<sub>8</sub>, which was 80%. There was no contribution from the deuterated standards to the unlabeled analytes arising from incomplete (*d*<sub>0</sub>) deuterium incorporation. HPLC grade water, methanol, and chloroform were purchased from Fisher Scientific (Pittsburgh, PA). Fatty acid free bovine serum albumin (BSA) was purchased from EMD Biosciences (San Diego, CA). Rat brain frontal cortex sections were provided by Dr. Ben Bahr at the University of Connecticut, Storrs.

**General Method of Synthesis: *N*-Acylethanolamides and Monoglycerides.** 1-(3-Dimethylaminopropyl)-3-ethylcarbodiimide

- (14) Rakhshan, F.; Day, T. A.; Blakely, R. D.; Barker, E. L. *J. Pharmacol. Exp. Ther.* **2000**, *292* (3), 960–7.
- (15) Rodriguez De Fonseca, F.; Gorriti, M. A.; Bilbao, A.; Escuredo, L.; Garcia-Segura, L. M.; Piomelli, D.; Navarro, M. *Neurotoxic. Res.* **2001**, *3* (1), 23–35.
- (16) Hanus, L.; Gopher, A.; Almog, S.; Mechoulam, R. *J. Med. Chem.* **1993**, *36* (20), 3032–4.
- (17) Hanus, L.; Abu-Lafi, S.; Fride, E.; Breuer, A.; Vogel, Z.; Shalev, D. E.; Kustanovich, I.; Mechoulam, R. *Proc. Natl. Acad. Sci. U.S.A.* **2001**, *98* (7), 3662–5.
- (18) Giuffrida, A.; Piomelli, D. *FEBS Lett.* **1998**, *422* (3), 373–6.
- (19) Di, Marzo, V.; Breivogel, C. S.; Tao, Q.; Bridgen, D. T.; Razdan, R. K.; Zimmer, A. M.; Zimmer, A.; Martin, B. R. *J. Neurochem.* **2000**, *75* (6), 2434–44.
- (20) Giuffrida, A.; Rodriguez de Fonseca, F.; Piomelli, D. *Anal. Biochem.* **2000**, *280*, (1), 87–93.
- (21) Bradshaw, H. B.; Rimmerman, N.; Krey, J. F.; Walker, J. M. *Am. J. Physiol. Regul. Integr. Comp. Physiol.* **2006**, *291*, (2), R349–58.

- (22) Bisogno, T.; Delton-Vandenbroucke, I.; Milone, A.; Lagarde, M.; Di, Marzo, V. *Arch. Biochem. Biophys.* **1999**, *370* (2), 300–7.
- (23) Sheskin, T.; Hanus, L.; Slager, J.; Vogel, Z.; Mechoulam, R. *J. Med. Chem.* **1997**, *40* (5), 659–67.
- (24) Watanabe, S.; Doshi, M.; Hamazaki, T. *Prostaglandins, Leukotrienes Essent. Fatty Acids* **2003**, *69* (1), 51–9.

hydrochloride (0.6 mmol) was added to a solution of fatty acid (0.5 mmol), ethanolamine, or glycerol (0.75 mmol), and *N,N*-dimethylaminopyridine (0.5 mmol) in 20 mL of acetonitrile at 0 °C. The reaction mixture was warmed to room temperature and stirred for 2–8 h. After the reaction was completed, as determined by TLC analysis (eluent, 30% acetone in hexane; stain developing agent, 5% phosphomolybdic acid in 95% ethanol), stirring was stopped and the solvent was evaporated under vacuum. The crude residue was loaded on SiO<sub>2</sub> and purified by the Biotage SP1 flash chromatography system (gradient method with acetone and hexane from 5 to 60%). Pure fractions were pooled, and the solvent was evaporated under vacuum to provide pure *N*-acylethanolamide/monoglyceride (75–90% yield) that was analyzed by NMR to ensure characteristic signals consistent with the assigned structures. The NMR assignment data for each endocannabinoid metabolite synthesized in-house can be found in the Supporting Information.

**Preparation of Standards.** Dried, purified samples of the 18 analytes and 18 deuterated analogues, ranging in weight from 1 to 5 mg, were diluted with an appropriate volume of ethanol to prepare separate 1 mg/mL stock solutions. The 200- $\mu$ L aliquots of each individual analyte stock solution were combined in a 15-mL Falcon tube (Beckton Dickson, Franklin Lakes, NJ) to form a 3.6-mL stock solution comprising all analytes and their labeled analogues. The 90- $\mu$ L aliquots of the combined stock solution were transferred to 40 individual 0.6-mL siliconized microcentrifuge tubes (Fisher Scientific). Each microcentrifuge tube contained 5000 ng of each analyte. The procedure was repeated with the 18 deuterated analogue stock solutions to generate 40 microcentrifuge tubes containing 5000 ng of each deuterated analog. The combined stock solution in each tube was evaporated to dryness under nitrogen at 30 °C (N-Evap 111, Organomation Associates, Berlin, MA). Upon dryness, each individual tube was capped, sealed with Parafilm (American National Can, Neenah WI), and stored at –80 °C until used for preparing calibration curves. A 20 mg/mL solution of fatty acid-free BSA was prepared by diluting 400 mg of BSA with 20 mL of water. The BSA solution was kept at 4 °C until analysis.

**Standard Curve Preparation.** On the day of analysis, a single vial of the dried analyte stock and a single vial of the dried deuterated analogue stock were reconstituted with 500  $\mu$ L of ethanol each to make 10 ng/ $\mu$ L working solutions. The 100  $\mu$ L of working analyte solution was diluted with 900  $\mu$ L of BSA in a 1.5-mL siliconized centrifuge tube (Fisher Scientific) to make a 1 ng/ $\mu$ L solution. A 100  $\mu$ L of the 1 ng/ $\mu$ L solution was further diluted with 900  $\mu$ L of BSA to make a 100 pg/ $\mu$ L solution of the combined analyte standard. A 1 ng/ $\mu$ L solution in BSA of the combined deuterated analogues was prepared in a manner identical to that for the 1 ng/ $\mu$ L analyte solution. Solutions of 1 ng/ $\mu$ L of both the combined analyte standard and the combined deuterated analogue standard were also prepared in ethanol, by a 1:10 dilution in ethanol of the 10 ng/ $\mu$ L working solutions. Aliquots of the 100 pg/ $\mu$ L and the 1 ng/ $\mu$ L BSA solutions were diluted with BSA solution to generate calibration standards of 0, 5, 10, 25, 50, 100, 250, 450, and 500 pg/ $\mu$ L. Twenty microliters of the 1 ng/ $\mu$ L deuterated analogue solution in BSA was added to each calibration standard to act as internal standard (IS). The total volume of each calibration standard was 200  $\mu$ L and contained 100 pg/ $\mu$ L of IS.

One extraction blank of 200  $\mu$ L of 20 mg/mL BSA solution was made. Quality control (QC) samples in BSA were made at analyte concentrations of 7, 21, 120, and 400 pg/ $\mu$ L and spiked with 20  $\mu$ L of 1 ng/ $\mu$ L IS in BSA. Three reference samples containing 300 pg/ $\mu$ L each of analyte and IS were prepared using the 1 ng/ $\mu$ L solutions in ethanol. Three reference extraction samples of the same concentration were also prepared using the 1 ng/ $\mu$ L solutions in BSA. QC and sample concentrations were calculated from the calibration curve using an equal weight linear regression (*X*) algorithm, where *X* represents concentration. The calibration curves were constructed from the ratios of the peak areas of the analytes versus the IS.

**Standard and Sample Extraction.** The extraction procedure for the calibration standards, QC, reference, and brain samples is modified from the Folch extraction.<sup>25</sup> The 50  $\mu$ L of ice cold PBS and 400  $\mu$ L of acetone were added to each calibration standard, blank extraction sample, and reference extraction sample, and then each mixture was vortexed for 10 s to precipitate protein. The samples were then centrifuged at 20800g for 5 min (Eppendorf Centrifuge 5417C, Hamburg Germany). The supernatant was transferred to a new 1.5-mL centrifuge tube and dried under nitrogen until the acetone was removed. A total of 100  $\mu$ L of PBS, 250  $\mu$ L of methanol, and 500  $\mu$ L of chloroform were added to the remaining supernatant, which was vortexed for 10 s, and then centrifuged at 20800g for 5 min to separate the two phases. The lower organic phase was transferred to a new 1.5-mL centrifuge tube and evaporated to dryness under nitrogen. The dried extracted standards were reconstituted in 200  $\mu$ L of ethanol, vortexed for 15 s, sonicated for 15 s, and then centrifuged at 20800g for 5 min before transferring them to HPLC vials for analysis.

Brain samples were received on dry ice and immediately stored at –80 °C until the following day when they were processed and analyzed. The frozen brain sections were weighed prior to homogenization in ice cold acetone/PBS, pH 7.4 (3:1) and 5  $\mu$ L of 1 ng/ $\mu$ L IS, followed by centrifugation at 10000g for 10 min at 4 °C. The resulting supernatant was dried under nitrogen until the acetone was removed. To the remaining supernatant, 100  $\mu$ L of PBS, one volume of methanol, and two volumes of chloroform were added for liquid–liquid-phase extraction of the lipids. The two phases were separated by centrifugation, and the bottom organic layer was evaporated to dryness under nitrogen. Brain extracts were reconstituted in 50  $\mu$ L of ethanol, vortexed, sonicated briefly, and centrifuged at 20800g for 5 min prior to analysis. In addition to the reconstituted sample, serial dilutions of 10 $\times$  and 100 $\times$  in ethanol prepared from each sample were also analyzed.

**LC–MS Analysis.** The liquid chromatography system used for analysis was an Agilent 1100 HPLC (Agilent Technologies, Wilmington DE). The autosampler was kept at 4 °C. Liquid chromatography was performed on a Zorbax SB-CN 2.1  $\times$  50 mm, 5- $\mu$ m, 80-Å column (Agilent Technologies). Mobile phase A consisted of 10 mM ammonium acetate, adjusted to pH 7.3 using ammonium hydroxide. Mobile phase B consisted of 100% methanol. Gradient elution was performed at a flow rate of 500  $\mu$ L/min. The initial composition of the gradient was 10% B. This was held

(25) Folch, J.; Lees, M.; Sloane Stanley, G. H. *J. Biol. Chem.* **1957**, 226 (1), 497–509.



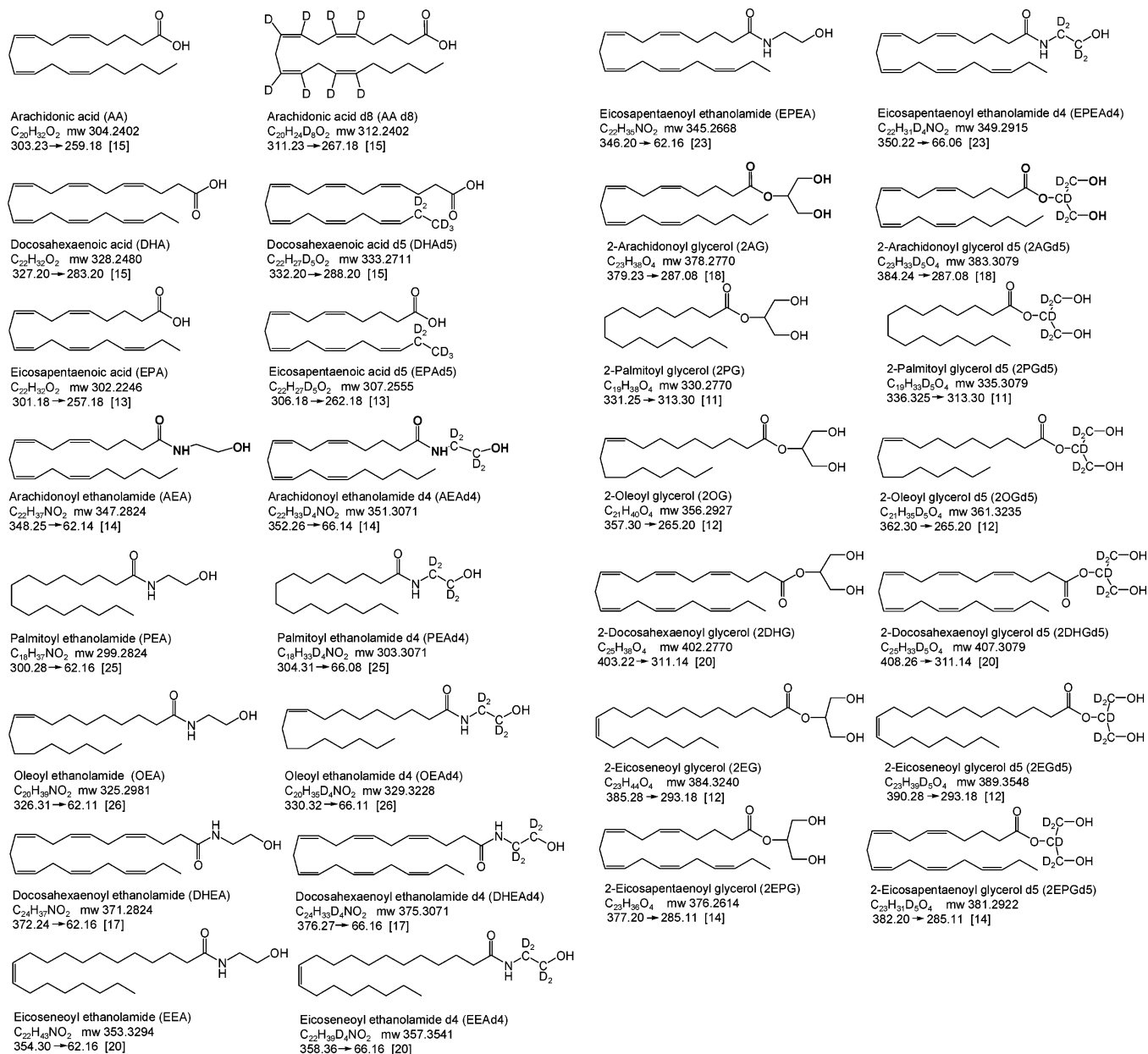


**Figure 1.** Structures of the endocannabinoid metabolites and their internal standards. Each analyte's SRM transition is listed in the last row of text. The specific collision energy used is shown in brackets.

isocratically for the first minute. At 1 min, mobile phase B increased to 60% B within 0.5 min. From 1.5 to 10 min, the gradient ramped linearly from 60% B to 75% B. At 10 min, the gradient increased to 95% B within 0.5 min, where it was held for 1.5 min. At 12.5 min, the gradient returned to initial conditions of 10% B to re-equilibrate the column. The total run time was 15 min. Chromatography was optimized to separate the free fatty acids during the first 6 min of the run and the ethanolamide and glyceride derivatives during the latter 9 min.

The column was connected to a TSQ Quantum Ultra-triple-quadrupole mass spectrometer (Thermo Fisher, San Jose CA). Analytes were ionized via APCI. The instrument was operated in both positive and negative ionization modes. During the first 6 min of the LC run, the Quantum operated in negative mode with a probe temperature of 380 °C, a source temperature of 250 °C, corona discharge current of 15  $\mu$ A, and a sheath gas setting of 30

psi. During the last 9 min of the LC run, the Quantum operated in positive mode with a probe temperature of 350 °C, a source temperature of 250 °C, corona discharge current of 6  $\mu$ A, and a sheath gas setting of 30 psi. For both ionization modes, the collision pressure was kept at 1 mTorr and centroid data were acquired. The resolution setting for Q1 and Q3 was 0.2, and each SRM scan time was 0.1 s. The SRM transitions that were monitored for each analyte and deuterated analogue are listed in Figure 1.

**Validation Procedure.** A validation program based on the FDA guidelines for linearity, inter- and intraday accuracy and precision, recovery, and stability was executed for the quantitation of the previously mentioned lipid modulators comprising the endocannabinoid metabolome.<sup>26</sup>

**Linearity.** Eight nonzero calibration standards, with analyte concentrations ranging from 5 to 500 pg/ $\mu$ L were prepared and

analyzed in triplicate in three separate analytical runs. The calibration curves were calculated by least-squares linear regression using an equal weighting factor. The standard concentrations were back-calculated from constructed calibration curves for each analyte. The deviation from nominal concentrations over three runs should be within  $\pm 15\%$  ( $\pm 20\%$  at the lower limit of quantitation) for the calibration standards.

**Accuracy and Precision.** The accuracy and precision of the assay were established by analyzing QC samples of each analyte. Three replicates of each sample were analyzed together with a complete set of calibration standards in three analytical runs. The intra-assay accuracy was determined as the percent difference between the mean concentration per analytical run and the nominal concentration. The interassay accuracy was determined as the percent difference between the mean concentration after three analytical runs and the nominal concentration. The coefficient of variation provided the measure of intra- and interassay precision. The accuracy and precision of the measured concentrations varied less than 15% from the nominal concentrations.

**Stability.** The stability of each analyte was investigated during all steps of the analysis, including the stability in the stock preparations in both ethanol and BSA over a 2-month period. Freeze–thaw stability of each analyte was also determined over four cycles at  $-80^\circ\text{C}$ . Analytes were considered stable in the biological matrix when 85–115% of the initial concentration was found. In stock solutions, analytes were considered stable when 90–110% of the initial concentration was found.

**Recovery.** The efficiency of the sample extraction procedure was determined by comparing the calculated concentrations of the nonextracted reference samples to the extracted reference samples. The percent recovery was calculated from the extracted/nonextracted ratio.

To support the use of BSA as the matrix for the preparation of standards, the extraction efficiency was also determined from rat brain homogenate by the method of standard additions. Briefly, several rat brains were homogenized following the exact procedure as described in the Standard and Sample Extraction section. The pooled homogenate was divided into three sets of five 1-mL aliquots. In each set, aliquots were spiked with 0, 2.5, 5.0, 12.5, and 25 ng of AEA, 2-AG, and EPA standards. Following sample extraction and reconstitution, the three sets were analyzed using the same LC–MS conditions described previously. The peak areas of each component were used to create the standard addition plot, from which the levels of each component were determined for each spiked aliquot. Subtraction of the endogenous level of each analyte from the spiked sample levels yielded the amount of spiked standard as determined by the standard additions method. The ratio of the measured spike amount to the true spike amount was used to determine the efficiency of the sample extraction.

## RESULTS AND DISCUSSION

**Method Development.** The structural diversity between the members of the endocannabinoid metabolome analyzed by the current method posed two main challenges to its success. First,

**Table 1. Sample Recovery Following Precipitation and Extraction Procedures**

analyte	reference sample		extraction recovery, %
	nonextracted	extracted	
AA	95.9	86.8	90.5
DHA	103.6	104.3	100.7
EPA	95.5	96.0	100.5
AEA	97.2	95.1	97.8
PEA	102.3	100.1	97.8
OEA	103.9	101.5	97.7
DHEA	101.6	101.5	99.9
EPEA	118.5	120.2	101.4
EEA	100.1	96.5	96.4
2AG	88.1	86.9	98.6
2PG	89.2	92.7	96.2
2OG	93.7	88.9	94.9
2DHG	89.8	92.2	102.7
2EPG	95.0	92.3	97.2
2EG	85.0	79.2	93.2

**Table 2. Extraction Recovery (Mean  $\pm$  SEM) of AEA, 2-AG, and EPA from Rat Brain Homogenate As Determined by the Standard Additions Method**

	regression $R^2$ value	extraction recovery, %
AEA	0.996	113.9 $\pm$ 24.1
2-AG	0.996	105.7 $\pm$ 22.0
EPA	0.959	96.4 $\pm$ 17.1

this method requires a mobile-phase system that would promote positive ionization of the ethanolamide and glycerol derivatives and negative ionization of the free acids by APCI conditions. In order to determine the effect of pH on ionization in both modes, several different additives, such as formic acid, acetic acid, ammonium hydroxide, methyl morpholine, and ammonium acetate, were studied. The type of organic solvent, either acetonitrile or methanol, was also tested to determine the best choice for ionization and elution strength. The best results were obtained using a 10 mM ammonium acetate pH 7.3 aqueous solution as solvent A and pure methanol as solvent B. Second, a chromatographic separation was required that could isolate the free acid metabolites from the ethanolamide and glyceride metabolites so that the ionization mode could be switched from negative to positive to ionize each component. Due to the hydrophobic character of all endocannabinoid metabolites, the retentiveness of typical C18 and C8 reversed-phase columns was too great to provide adequate separation. However, the cyano column, with its low retention and alternative selectivity, was able to separate the components with enough resolution to operate the method in both modes successfully.

With a suitable solvent system and chromatographic separation established, precursor and product ions for each analyte were determined by direct infusion. The most intense product ion was monitored for each analyte. Choosing the best product ion fragment for each SRM transition was complicated because the core fatty acid tails tended to fragment into many different products. However, characteristic losses from each of the derivative types were exploited and suitable product ions were determined. For the ethanolamide derivatives, fragmentation of the amide bond between the fatty acid core and the ethanolamine

(26) Food and Drug Administration (FDA) Guidance for Industry—Bioanalytical Method Validation, 2001; <http://www.fda.gov/guidance/4252fnl.htm> (accessed June 2007).

**Table 3. Inter- and Intraday Accuracy and Precision of the QC Sample at Four Concentrations<sup>a</sup>**

analyte		QC 1: 7 pg/ $\mu$ L			QC 2: 21 pg/ $\mu$ L			QC 3: 120 pg/ $\mu$ L			QC 4: 400 pg/ $\mu$ L		
		mean	accuracy, %	precision, %	mean	accuracy, %	precision, %	mean	accuracy, %	precision, %	mean	accuracy, %	precision, %
AEA	intraday 1	6.6	6	11.8	20.9	0.4	3.2	115.5	3.8	3.1	392.0	2.0	5.1
	intraday 2	6.8	2.5	3.1	20.3	3.2	3.8	111.8	6.9	1.5	388.4	2.9	4.2
	intraday 3	7.1	1.1	16.3	21.0	0.1	3.5	123.0	2.5	1.5	408.8	2.2	3.2
	interday	6.8	3.2	10.4	20.7	1.2	3.5	116.8	4.4	2.0	396.4	2.4	4.2
PEA	intraday 1	6.8	3.2	5.6	21.3	1.5	3.3	119.2	0.6	7.0	390.4	2.4	5.6
	intraday 2	7.2	3.5	2.9	20.3	3.5	8.6	114.5	4.6	3.8	400.6	0.1	6.0
	intraday 3	6.9	1	9.1	21.8	3.7	2.0	120.3	0.3	2.1	403.5	0.1	1.1
	interday	7.0	2.6	5.9	21.1	2.9	4.6	118.0	1.8	4.3	398.2	0.9	4.2
OEA	intraday 1	6.8	3.3	3.7	20.6	2.0	2.0	124.8	4.0	7.0	388.7	2.8	2.6
	intraday 2	6.9	2	1.7	21.4	2.0	3.2	115.8	3.5	2.4	407.8	2.0	3.0
	intraday 3	7.4	5.8	7.9	20.1	4.1	6.0	121.4	1.1	0.4	390.4	2.4	3.4
	interday	7.0	3.7	4.4	20.7	2.7	3.7	120.7	2.9	3.3	395.6	2.4	3.0
DHEA	intraday 1	6.7	4.6	7.9	21.9	4.5	3.9	125.9	4.9	2.9	410.1	2.5	4.8
	intraday 2	6.7	3.7	9.3	21.2	1.2	5.5	110.3	8.1	1.2	390.2	2.5	1.0
	intraday 3	7.0	0.5	6.6	21.0	0.2	4.7	120.4	0.4	0.9	392.9	1.8	1.4
	interday	6.8	2.9	7.9	21.4	2.0	4.7	118.9	4.5	1.7	397.7	2.3	2.4
EPEA	intraday 1	6.8	3.1	11.2	19.0	5.0	8.2	134.6	12.1	5.4	431.6	7.9	2.9
	intraday 2	6.0	14.7	10.6	19.1	4.3	13.3	123.2	2.7	3.2	424.5	6.1	6.6
	intraday 3	7.5	7.0	7.4	19.8	1.1	5.4	130.3	8.6	2.0	423.1	5.8	2.1
	interday	6.7	8.3	9.7	19.3	3.4	9.0	129.4	7.8	3.5	426.4	6.6	3.9
EEA	intraday 1	6.9	1.3	4.3	20.9	0.4	3.7	120.2	0.1	5.3	407.3	1.8	9.0
	intraday 2	6.5	7.7	7.5	20.9	0.4	1.0	116.3	3.1	3.1	401.0	0.2	6.0
	intraday 3	7.1	1.5	2.6	20.8	0.9	3.4	123.2	2.7	3.1	397.4	0.7	2.0
	interday	6.8	3.5	4.8	20.9	0.5	2.7	119.9	2.0	3.8	401.9	0.9	5.6
2AG	intraday 1	6.6	6.1	12.8	21.8	3.8	6.5	121.6	1.3	0.2	376.2	6.0	4.3
	intraday 2	6.9	1.0	13.1	17.9	14.8	10.2	111.5	7.1	13.8	428.8	7.2	12.9
	intraday 3	5.8	17.7	7.9	18.4	12.2	4.3	119.4	0.5	11.7	380.4	4.9	5.0
	interday	6.4	8.3	11.3	19.4	10.3	7.0	117.5	3.0	8.6	395.1	6.0	7.4
2PG	intraday 1	6.3	9.8	8.2	20.5	2.3	6.3	116.4	3.0	3.2	408.4	2.1	2.3
	intraday 2	6.8	2.9	6.7	22.8	8.6	5.8	121.8	1.5	5.4	415.6	3.9	2.6
	intraday 3	5.7	18.5	12.3	21.7	8.1	9.4	107.4	10.5	8.2	418.3	4.6	7.4
	interday	6.3	10.4	9.1	21.7	6.3	7.2	115.2	5.0	5.6	414.1	3.5	4.1
2OG	intraday 1	7.2	3.4	5.1	20.5	2.5	7.5	122.6	2.1	11.1	390.4	2.4	10.2
	intraday 2	6.9	0.8	13.3	19.1	8.9	2.3	122.8	2.3	4.7	428.5	7.1	1.5
	intraday 3	7.4	6.1	8.1	22.2	5.7	9.9	130.7	8.9	13.2	408.8	2.2	2.8
	interday	7.2	3.4	8.8	20.6	5.7	6.6	125.4	4.4	9.7	409.2	3.9	4.8
2DHG	intraday 1	6.6	6.0	7.9	23.6	12.5	11.3	127.4	6.2	2.2	368.2	7.9	0.6
	intraday 2	7.2	2.3	14.7	22.3	6.3	3.6	117.4	2.1	0.8	394.5	1.3	4.5
	intraday 3	6.3	10.4	12.4	21.3	1.6	5.2	117.6	2.0	4.0	399.5	0.1	5.0
	interday	6.7	6.2	11.7	22.4	6.8	6.7	120.8	3.4	2.3	387.4	3.1	3.4
2EPG	intraday 1	7.4	5.5	5.6	23.3	11.8	9.1	119.7	0.3	9.4	383.4	4.2	7.2
	intraday 2	6.6	5.5	13.5	18.0	14.1	7.5	119.9	0.1	7.8	443.2	10.8	14.8
	intraday 3	7.3	4.3	13.9	20.1	4.4	8.2	124.5	3.7	8.6	405.7	1.4	11.6
	interday	7.1	5.1	11.0	20.5	10.1	8.3	121.4	1.4	8.6	410.8	5.5	11.2
2EG	intraday 1	6.9	1.6	8.5	22.1	5.0	3.9	108.7	9.5	2.6	392.0	2.0	2.0
	intraday 2	7.3	4.2	12.9	23.2	10.4	8.0	121.5	1.2	7.5	405.5	1.4	10.0
	intraday 3	7.3	4.6	8.3	18.7	10.7	12.7	116.5	2.9	10.4	424.3	6.1	10.7
	interday	7.2	3.5	9.9	21.3	8.7	8.2	115.6	4.5	6.9	407.3	3.2	7.6
AA	intraday 1	5.9	16.1	1.3	18.6	11.6	7.3	110.5	7.9	6.4	392.7	1.8	7.1
	intraday 2	6.6	5.3	1.9	18.4	12.2	2.0	111.3	7.2	8.7	386.9	3.2	5.7
	intraday 3	5.8	16.6	14.7	21.4	1.8	12.7	123.1	2.5	1.3	396.1	1.0	7.3
	interday	6.1	12.7	6.0	19.5	8.5	7.3	115.0	5.9	5.5	391.9	2.0	6.7
DHA	intraday 1	7.7	10.4	13.2	21.1	0.5	6.9	119.5	4.1	9.8	384.5	3.9	5.6
	intraday 2	5.8	17.6	19.7	20.9	0.3	10.6	121.6	1.3	4.2	410.8	2.7	2.8
	intraday 3	8.1	16.4	8.0	21.1	0.5	17.1	118.0	1.6	0.8	420.1	5.0	4.6
	interday	7.2	14.8	13.6	21.0	0.4	11.5	119.7	2.3	4.9	405.1	3.9	4.3
EPA	intraday 1	6.7	4.3	1.2	20.3	3.1	8.9	108.0	10.0	2.7	417.8	4.4	2.5
	intraday 2	6.10	12.3	6.1	20.1	4.4	8.1	119.3	0.6	2.6	401.3	0.3	5.7
	intraday 3	6.80	2.4	13.3	20.3	3.5	3.8	122.5	2.1	9.3	386.1	3.5	2.7
	interday	6.5	6.3	6.9	20.2	3.7	6.9	116.6	4.2	4.9	401.7	2.7	3.6

<sup>a</sup> Accuracy % represents the difference between the measured and true value. Precision % represents the average standard deviation of the measurements ( $n = 3$ ).

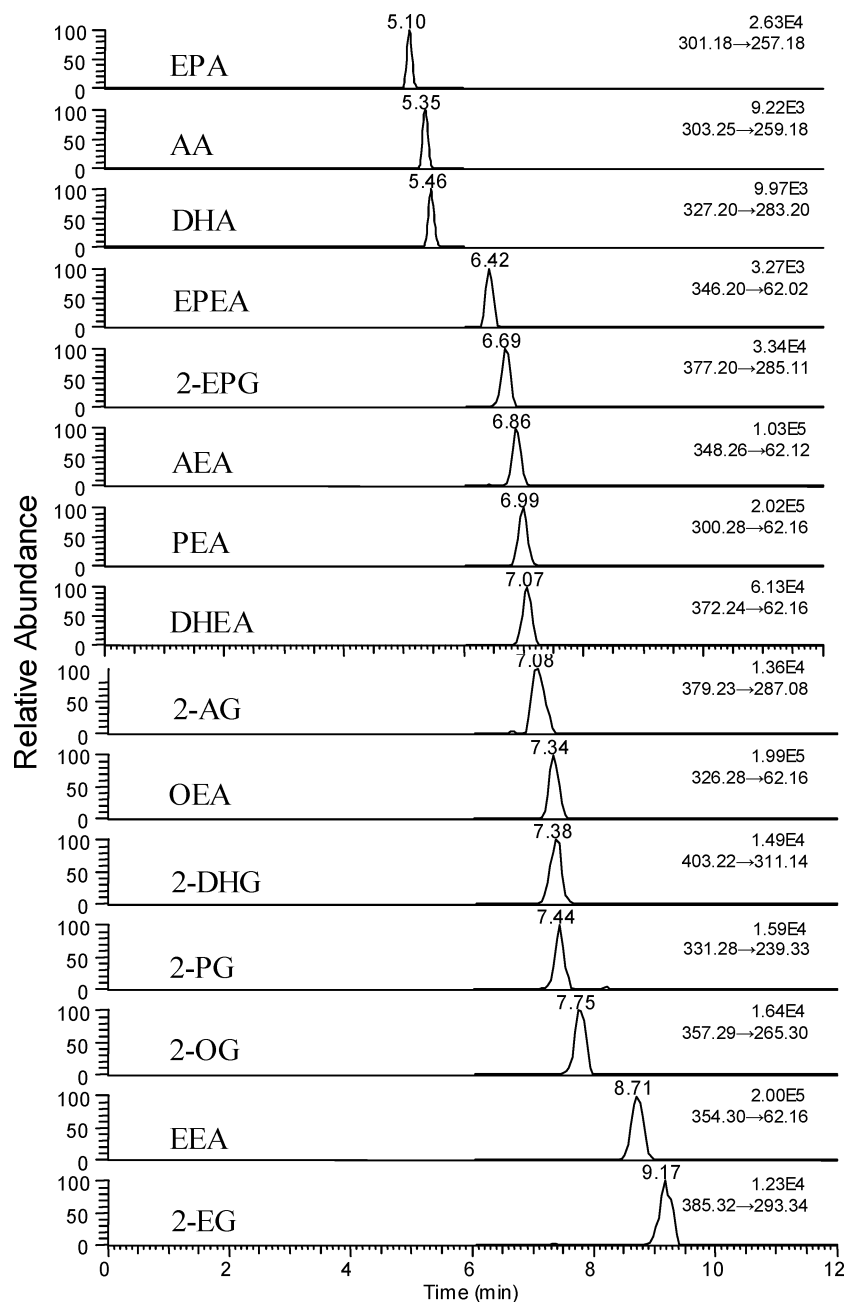


**Figure 2.** Extracted MRM chromatograms of the endocannabinoid metabolites in the reference standard, 500 pg of each analyte on column.

yielded protonated ethanolamine products of  $m/z$  62. Internal standards for these metabolites are labeled with four deuteriums on the ethanolamine tail, resulting in a product ion of  $m/z$  66.2. In a fashion similar to the ethanolamides, the glyceride derivatives fragmented at the ester linkage between the fatty acid and the glyceride moiety. However, in these cases, the charge was typically retained on the fatty acid core, giving product ions that were 91 amu less than the precursor  $m/z$ . Since the internal standards of the glyceride derivatives were labeled on the glycerol moiety itself, the resulting product ions had the same  $m/z$  as the unlabeled precursors. We investigated whether cross talk arising from monitoring the same product ion  $m/z$  for both the analyte and internal standard would affect instrument response. A comparison of absolute peak areas of unlabeled 2-AG and its internal standard 2-AG $d_5$  showed that there was no significant difference in area for either analyte when run separately, in a 1:1

ratio or in a 5:1 2-AG/2-AG $d_5$  ratio. We therefore concluded that cross talk was not a factor in the analysis.

Determining the optimal product ion for the SRM transitions of the free fatty acids was difficult because of the absence of chemical moieties whose cleavage would result in a predominant fragment. In negative mode APCI, the product ion fragment we monitored was the decarboxylation product of the fatty acid, corresponding to a loss of 44 amu. The transitions worked well for AA, DHA, and EPA, due to the relatively large number of double bonds (4, 6, and 5, respectively) that could support a negative charge. However, the sensitivity of PA, OA, and EA (0, 1, and 1 double bond, respectively) under these conditions was too poor for this analysis. We therefore decided not to include them in this study.

Although the free acids of palmitic, oleic, and eicosenoic acid were not included in the analysis, their respective ethanolamide

**Table 4. Endocannabinoid Stability in Ethanol and BSA (%) over 2-Months Storage at  $-80^{\circ}\text{C}$  and Four Freeze–Thaw Cycles**

analyte	ethanol single thaw				ethanol multiple thaw				BSA single thaw				BSA multiple thaw			
	day 1	week 1	month 1	month 2	day 1	week 1	month 1	month 2	day 1	week 1	month 1	month 2	day 1	week 1	month 1	month 2
AA	94.1	95.3	96.8	57.7	109.6	96.0	102.7	55.4	100.4	93.9	93.9	56.8	105.0	91.4	99.3	52.5
DHA	93.1	94.5	99.7	107.1	94.9	94.3	99.6	118.0	95.2	90.6	101.4	104.2	93.3	94.3	93.5	109.0
EPA	101.	101.3	88.3	93.9	98.7	103.5	90.7	96.2	100.5	101.5	81.3	96.4	98.5	96.6	95.2	99.4
AEA	100.7	98.8	98.6	90.3	106.4	98.6	103.1	94.8	102.8	97.7	103.5	96.5	102.4	100.6	100.3	91.6
PEA	101.4	98.4	98.9	88.8	97.8	97.6	100.9	89.9	100.4	96.7	97.5	86.2	100.1	96.1	97.9	88.3
OEA	97.8	99.4	97.3	92.6	102.5	99.0	98.7	87.4	103.2	94.9	99.6	90.8	100.6	98.8	95.6	88.5
DHEA	96.1	96.2	98.7	102.4	95.6	91.5	102.2	95.2	97.3	95.0	99.3	98.9	106.2	92.6	97.7	91.3
EPEA	99.1	88.1	104.2	99.1	101.1	89.9	99.1	110.2	92.0	90.2	99.6	105.0	89.4	90.0	99.6	97.3
EEA	107.0	94.2	97.1	95.9	102.7	100.6	103.1	103.7	102.1	97.9	98.8	97.4	100.5	98.8	97.1	102.1
2AG	93.9	98.5	101.9	107.8	89.3	93.9	97.6	109.7	84.6	89.0	98.9	102.0	92.9	93.2	99.2	96.8
2PG	97.6	99.2	96.8	96.5	101.2	98.4	98.5	95.3	98.5	98.3	98.9	95.2	103.2	100.2	98.7	93.1
2OG	120.7	95.1	105.3	102.9	123.8	98.4	83.4	102.1	109.1	105.6	87.5	111.1	118.8	89.1	84.	106.0
2DHG	101.9	94.0	88.2	97.0	104.2	105.6	92.4	97.8	112.2	111.2	91.9	98.2	114.6	100.3	99.5	88.7
2EPG	102.7	102.7	95.4	89.6	102.9	92.3	96.0	103.4	93.3	97.4	102.5	88.7	100.6	90.9	96.5	89.9
2EG	99.4	99.3	96.4	89.3	98.6	97.8	99.4	96.2	97.8	96.2	101.1	94.3	99.4	99.1	98.9	88.2

and glyceride derivatives were. The structure of each metabolite and its internal standard are shown in Figure 1. In addition, the text accompanying each structure includes its formula and molecular weight as well as the SRM transition and collision energy used in the analysis.

**Validation.** The endocannabinoids and related lipid mediators are produced endogenously and are present in the brain and plasma. Therefore, it is not possible to use plasma as the matrix for preparing calibration standards, since the endocannabinoids' baseline levels in plasma would alter the known calibration amounts. To mimic as closely as possible the plasma and brain matrixes, we chose to use a solution of BSA, the most abundant protein in plasma, which had been stripped of its fatty acid component. Based on results obtained from a Bradford assay (Pierce Biotechnology, Rockford, IL), we found the level of total protein in mouse brain homogenate to be 20 mg/mL. This level was chosen as the concentration of "fatty acid-free" BSA to use as our standard matrix. In order to ensure that there was no contribution from the BSA matrix to the measured levels of endocannabinoids, a series of blanks were run to ascertain possible interference. The results for the ethanol blank, the BSA extracted matrix blank, and a BSA extracted matrix spiked with internal standard only (standard A) confirmed that the matrixes did not contain any detectable levels of endocannabinoids.

The recovery of each analyte from the matrix following the protein precipitation and liquid extraction steps was determined in order to measure the efficiency of the extraction. Reference samples were prepared with 100 pg/ul each of standard and internal standard in ethanol and 20 mg/mL BSA matrix. The ethanol reference standard was injected without extraction while the BSA reference standard was extracted following the procedure outlined in the Experimental Section. The amounts of nonextracted and extracted reference standards were back-calculated from the calibration curves for each analyte, and the percent recovery was calculated from the extracted/nonextracted ratio. Table 1 lists the percent recovery after sample workup for each endocannabinoid studied. The recovery values ranged from 90.5 to 102.7%, indicating high extraction efficiency. Comparisons of

absolute peak areas for extracted/nonextracted samples were also within 10–15% (not shown).

In order to confirm the validity of using BSA as a substitute matrix for actual brain tissue during sample preparation, the method of standard additions, which can quantify endogenous analytes by direct internal calibration using the true sample matrix rather than through external calibration, was performed using AEA, 2-AG, and EPA. These analytes were chosen to represent the entire group of endocannabinoid metabolites based on their differences in relative abundance and chemical functionality. Analyte peak areas at each level were plotted against the spike amount and the resulting best fit curve was back-extrapolated to the  $x$ -intercept to determine the endogenous level of analyte present. The endogenous level was subtracted from the measured spiked amount and then compared to the actual spiked amount to determine the extraction efficiency. Table 2 reports the percent recovery and the  $R^2$  value of the best-fit curve obtained for AEA, 2-AG, and EPA. The percent extraction recovery is an average of triplicate measurements. The percent recoveries from rat brain homogenate are slightly higher for the three analytes compared to their recoveries from the BSA matrix. Direct comparison shows that the recoveries are within 15% variation of each other and demonstrates that it is reasonable to use BSA as an alternative sample matrix to brain homogenate.

The linearity of the method over the concentration range of 5–500 pg/ $\mu\text{L}$  was determined by the calibration curves constructed for each analyte. Curves plotted the ratio of the analyte area to its internal standard area against concentration. No weighting factors were used to bias either end of the best-fit linear curve through the data points. Regression analysis determined  $R^2$  values of 0.99 or greater for each analyte. The lower limit of quantitation, the amount of sample required to give a signal-to-noise (S/N) ratio of 10 or greater, was determined to be 25 pg on column for each analyte. Similarly, the limit of detection, the amount of sample required to give a S/N ratio of 3 or better, was  $\sim 10$  pg on column for each analyte. Figure 2 shows the extracted ion chromatogram for each transition monitored. The analytes are displayed in the order of their elution from the column.



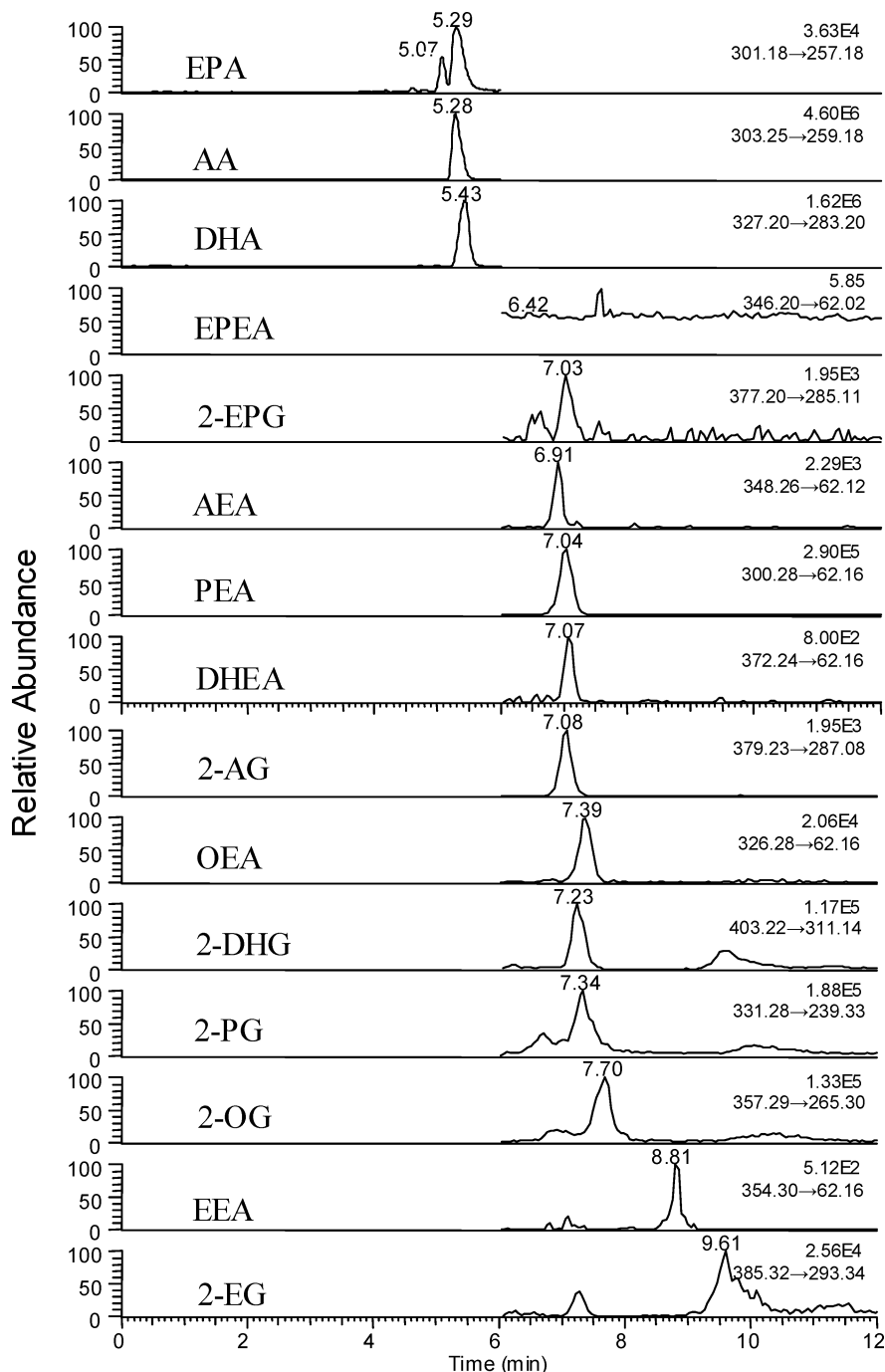


**Figure 3.** Extracted endocannabinoid MRM chromatograms from rat frontal cortex. Each chromatogram has been normalized to display the peak of maximum intensity within the time window.

Arachidonic, docosahexaenoic, and eicosapentaenoic acids elute within the first 6 min. The polarity switches from APCI− to APCI+ at 6 min to detect the ethanolamide and glyceride derivatives of the six core fatty acids described in the Experimental Section.

Table 3 lists the accuracy and precision data acquired for intraday and interday analyses. The accuracy and precision were determined using QC samples prepared at four concentrations spanning the entire concentration range measured by the method. The concentrations of QC samples 1, 2, 3, and 4 were 7, 21, 120, and 400 pg/ul, respectively. Triplicate injections of each QC sample were made three times daily over the course of 24 h to determine the method's intraday variability. The QC sample mean

value for each run was obtained by averaging the back-calculated amounts of the triplicate injections for each of the three analyses made during 1 day. Accuracy was calculated as the percent difference between the daily mean QC value and the true value. Precision was calculated as the percent standard deviation of the three daily values. To determine the interday variability of the method, the accuracy and precision of runs 1–3 were averaged. New calibration curves were run each day in conjunction with the QC samples. The mid- to high-level QC samples (QC 2–QC 4) for each component had greater than 85% accuracy and precision while the low QC 1 sample's accuracy and precision was greater than 80%. These levels meet the acceptance criteria

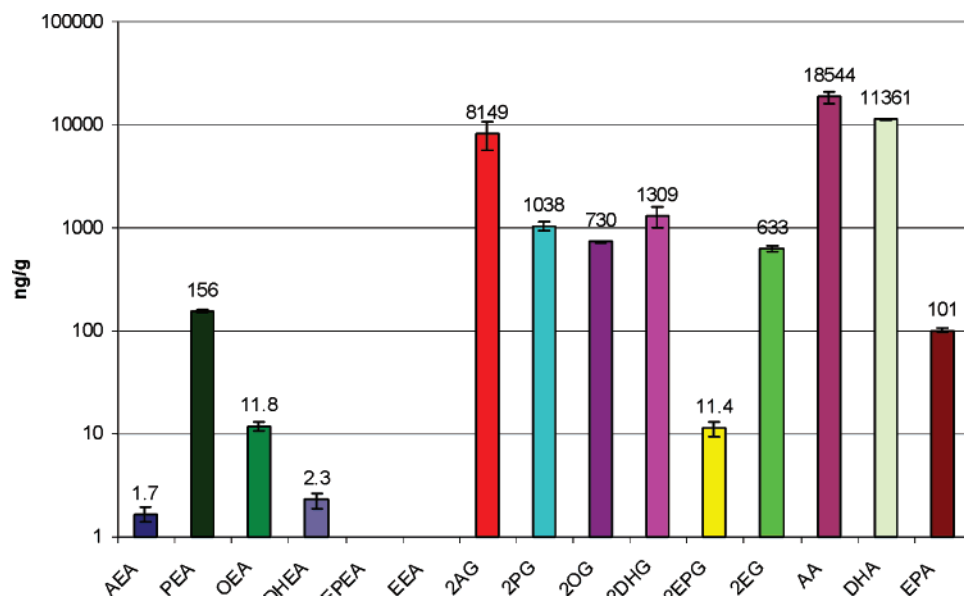


**Figure 4.** Endocannabinoid metabolomic profile of rat frontal cortex.

outlined in the validation guidelines. The majority of samples had accuracy and precision greater than 90%, indicating that the method can be considered accurate and precise across the range of concentrations used.

The stability of the endocannabinoid metabolites was studied in both ethanol and BSA over 2 months at  $-80^{\circ}\text{C}$ . Aliquots from each matrix were analyzed following 1 day, one week, 1 month, and 2 months. For each time point, two sets of samples initially were prepared that served as single and multiple thaw sets. Therefore, the analysis on day one consisted of two sets each thawed just once. Within 2 months, the multiple thaw sample set had cycled through four freeze/thaws, corresponding to one freeze/thaw for each time point analyzed. The single thaw set had been maintained at  $-80^{\circ}\text{C}$  for the full 2 months. The results are listed in Table 4, which shows the percent of each metabolite remaining in solution for the specific matrix, time, and freeze/thaw point. For each time point, fresh calibration curves and reference samples for each metabolite were compared to the stability samples. The stability samples were spiked with fresh internal standard prior to analysis for an accurate reflection of peak area ratio differences. The majority of the metabolites at each time point were within 15% of the reference sample level. The one metabolite that degraded significantly by the second month was arachidonic acid. In both ethanol and BSA, the levels had dropped to between 50 and 60% of the reference sample. The levels were similar in the multiple thaw samples. Due to the instability of AA at 2 months, the endocannabinoid stock solutions were prepared fresh once per month to maintain sample integrity. The metabolites are stable through four cycles of freeze–thaw.

**Analysis of Biological Samples.** To demonstrate the method's applicability for quantifying the endocannabinoid metabolome, rat brain frontal cortex regions were analyzed. Briefly, two groups of Sprague-Dawley rats ( $n = 3$  in each group) were dosed intraperitoneally with either vehicle or 8 mg/kg palmitylsulfonyl fluoride (AM374). AM374 is a known inhibitor of the enzyme FAAH, fatty acid amide hydrolase, that hydrolyzes *N*-acyl etha-

nolamides into carboxylic acids and ethanolamine.<sup>27</sup> FAAH acts as one of the main regulatory enzymes associated with the hydrolysis of the endocannabinoid anandamide.<sup>28</sup> Treatment with AM374 was expected to inhibit the degradation of anandamide within the brain and elevate the level of anandamide, compared to vehicle treatment. Figure 3 shows an example of the extracted MRM chromatograms obtained from rat frontal cortex homogenate. Matching each endocannabinoid's retention time to its internal standard was performed to ensure that the correct peak in each chromatogram was integrated properly. Small deviations in retention times between reference standards (Figure 2) and brain homogenate (Figure 3) are paralleled by corresponding deviations of each endocannabinoid's internal standard. The acyl glycerol derivatives exhibit a slightly distorted peak shape due to the partial chromatographic resolution of the *sn*-2 isomer from the *sn*-1 or *sn*-3 isomers. Since this method does not fully resolve each isomer, reported acyl glycerol levels include quantification of all isomers. Figure 4 shows the profile of the endocannabinoid metabolome as measured in the frontal cortex of the rat vehicle samples. The levels of individual metabolites vary over 4 orders of magnitude and as such are presented on a logarithmic scale. AEA was the lowest quantifiable metabolite at 1.7 ng/g of wet tissue, while the level of AA was 18.5  $\mu\text{g/g}$ . EEA was detected but was below the limit of quantitation for the analysis. EPEA was not detected at all. The levels of AEA, 2-AG, OEA, and PEA found in mouse brain are within the range reported by others.<sup>19,29–31</sup>

(27) Deutsch, D. G.; Lin, S.; Hill, W. A.; Morse, K. L.; Salehani, D.; Arreaza, G.; Omeir, R. L.; Makriyannis, A. *Biochem. Biophys. Res. Commun.* **1997**, *231* (1), 217–21.

(28) Egertova, M.; Cravatt, B. F.; Elphick, M. R. *Neuroscience* **2003**, *119* (2), 481–96.

(29) Baker, D.; Pryce, G.; Croxford, J. L.; Brown, P.; Pertwee, R. G.; Makriyannis, A.; Khanolkar, A.; Layward, L.; Fezza, F.; Bisogno, T.; Di Marzo, V. *FASEB J.* **2001**, *15* (2), 300–2.

(30) Cravatt, B. F.; Demarest, K.; Patricelli, M. P.; Bracey, M. H.; Giang, D. K.; Martin, B. R.; Lichtman, A. H. *Proc. Natl. Acad. Sci. U.S.A.* **2001**, *98* (16), 9371–6.

(31) Franklin, A.; Parmentier-Batteur, S.; Walter, L.; Greenberg, D. A.; Stella, N. J. *Neurosci.* **2003**, *23* (21), 7767–75.

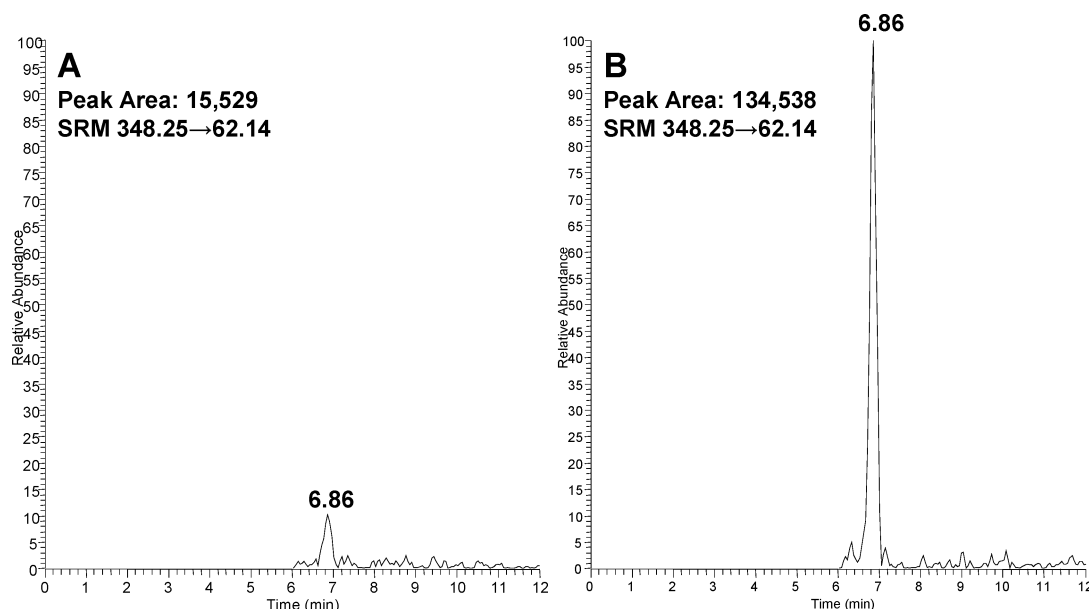


**Figure 5.** Extracted chromatogram of AEA in rat frontal cortex treated with (A) vehicle or with (B) FAAH inhibitor AM374.

The levels of the other acyl glycerol and acyl ethanolamine metabolites determined in this study have not been reported. This profile shows that metabolite levels for an individual core structure are lowest for the ethanolamide derivative and increase for the glyceride derivatives and free acids. Due to the greater abundance of the *N*-acyl glycerols, such as 2-AG or 2-PG, over the *N*-acyl ethanolamines, these glyceride derivatives may contribute more to the physiological effects of endocannabinoids than the *N*-acyl ethanolamines (such as AEA) even though cannabinoid receptor binding affinity may favor the lesser component.

Figure 5A and Figure 5B are representative extracted ion chromatograms of AEA from the rat frontal cortex analysis that correspond to treatments with the vehicle and AM374, respectively. The sample time point in Figure 5B is 3 h after administering AM374. A comparison of the peak areas shows a 9-fold increase in AEA levels between the two samples. The calculated AEA levels between the untreated and treated frontal cortex samples were 0.64 and 7.50 ng/g, respectively. These data indicate that treating with the FAAH inhibitor AM374 causes a significant increase in AEA levels in the frontal cortex. A comprehensive study is currently being completed that monitors endocannabinoid levels following AM373 treatment at several times and at several locations in rat brain using the presently developed method. Correlations between the neuroprotective properties of AM374, animal behavior, and changes in the entire endocannabinoid metabolome will be presented.

## CONCLUSIONS

In this paper, we describe the development, validation, and application of a quantitative assay to profile the levels of several members of the endocannabinoid metabolome by LC-APCI-MS-MS. The endocannabinoids are an important group of endogenous ligands for the cannabinoid system of receptors and enzymes whose complete biological significance is currently under intense investigation. The need for a thorough evaluation of the endocannabinoid metabolome was also illustrated in a recent publication, which came to our attention during the preparation of this article.<sup>32</sup>

The paper reports on the simultaneous analysis of eight metabolites using LC-ESI-MS but employs only two internal standards for quantifying the entire set of metabolites. Differences in the selected metabolites' ionization efficiency due to differences in chemical structure and chromatographic elution favor the use of separate internal standards for each metabolite for improved quantitative accuracy. The current endeavor effectively doubles the number of endocannabinoids that can be quantified simultaneously, allowing for a more comprehensive endocannabinoid metabolomic profile to be established. The validation criteria established for bioanalytical methodology have been met for several important parameters. Linearity based upon regression constants greater than 0.99 were obtained for each metabolite, over the calibration range of 25 pg to 2.5 ng on column. The absence of interferences tested in a series of blanks at the chosen MRM transitions demonstrated the specificity of the methodology. The accuracy, precision, and ruggedness of the method were established by examining the reproducibility of several QC samples over extended times and conditions. Finally an endocannabinoid profile for the rat frontal cortex has been established and the variations in anandamide level due to treatment with the FAAH inhibitor AM374 have been quantified successfully. The potential benefit of establishing known endocannabinoid profiles extends far beyond the rat model used in this study. The endocannabinoid system may play a significant role in human disease pathologies ranging from neurological disorders such as schizophrenia and postpartum depression to cannabinoid abuse and dependence. Additionally, several cannabinergic xenobiotics have been developed by this group and others that target key endocannabinoid proteins and modulate the composition of the endocannabinoid metabolome. Thus, determination of the levels of endocannabinoid metabolites under diverse physiological conditions provides an excellent window of information on the physiological system being studied. As novel endocannabinoids con-

(32) Richardson, D.; Ortori, C. A.; Chapman, V.; Kendall, D. A.; Barrett, D. A. *Anal. Biochem.* **2007**, *360* (2), 216–26.

tinue to be discovered, it is necessary to further develop the quantitation methodology. We are currently working on high-throughput methodologies with greater sensitivity to tackle the rapidly expanding endocannabinoid metabolome.

#### **ACKNOWLEDGMENT**

This research was supported by grants from the National Institutes of Health, DA-91587215 and DA-91583801.

#### **SUPPORTING INFORMATION AVAILABLE**

NMR structural assignments for all endocannabinoid metabolites synthesized in-house. This material is available free of charge via the Internet at <http://pubs.acs.org>.

Received for review December 20, 2006. Accepted May 24, 2007.

AC0624086